

# Probing the Transition-State Structure of Dual-Specificity Protein Phosphatases Using a Physiological Substrate Mimic<sup>†</sup>

Piotr K. Grzyska,<sup>‡,§</sup> Youngjoo Kim,<sup>‡,||</sup> Michael D. Jackson,<sup>||</sup> Alvan C. Hengge,<sup>\*,§</sup> and John M. Denu<sup>\*,⊥</sup>

Chemistry and Biochemistry, Utah State University, Logan, Utah 84322, Biochemistry and Molecular Biology, Oregon Health and Science University, Portland, Oregon 97239, and Biomolecular Chemistry, University of Wisconsin, Madison, Wisconsin 53706

Received March 16, 2004; Revised Manuscript Received May 7, 2004

**ABSTRACT:** Dual-specificity phosphatases (DSPs) belong to the large family of protein tyrosine phosphatases that contain the active-site motif (H/V)CxxGxxR(S/T), but unlike the tyrosine-specific enzymes, DSPs are able to catalyze the efficient hydrolysis of both phosphotyrosine and phosphoserine/threonine found on signaling proteins, as well as a variety of small-molecule aryl and alkyl phosphates. It is unclear how DSPs accomplish similar reaction rates for phosphoesters, whose reactivity (i.e.,  $pK_a$  of the leaving group) can vary by more than  $10^8$ . Here, we utilize the alkyl phosphate *m*-nitrobenzyl phosphate (*m*NBP), leaving-group  $pK_a = 14.9$ , as a physiological substrate mimic to probe the mechanism and transition state of the DSP, *Vaccinia H1*-related (VHR). Detailed pH and kinetic isotope effects of the *V/K* value for *m*NBP indicates that VHR reacts with the phosphate dianion of *m*NBP and that the nonbridge phosphate oxygen atoms are unprotonated in the transition state. <sup>18</sup>O and solvent isotope effects indicate differences in the respective timing of the proton transfer to the leaving group and P–O fission; with the alkyl ester substrate, protonation is ahead of P–O fission, while with the aryl substrate, the two processes are more synchronous. Kinetic analysis of the general-acid mutant D92N with *m*NBP was consistent with the requirement of Asp-92 in protonating the ester oxygen, either in a step prior to significant P–O bond cleavage or in a concerted but asynchronous mechanism in which protonation is ahead of P–O bond fission. Collectively, the data indicate that VHR and likely all DSPs can match leaving-group potential with the timing of the proton transfer to the ester oxygen, such that diverse aryl and alkyl phosphoesters are turned over with similar catalytic efficiency.

Dual-specificity phosphatases (DSPs)<sup>1</sup> constitute a large subfamily of the protein tyrosine phosphatases (PTPs). While PTPs dephosphorylate phosphotyrosine residues, DSPs efficiently dephosphorylate all three major types of phosphorylated residues found in eukaryotes: phosphoserine, phosphothreonine, and phosphotyrosine. Many DSPs downregulate mitogen-activated protein kinases (MAPKs) by hydrolyzing phosphothreonine and phosphotyrosine residues within the activation loop TxY motif (3, 4). Although there is sparse sequence identity between the PTPs and DSPs, both families share a similar overall structure and general catalytic mechanism (5, 6). Utilizing the active-site motif (H/V)-

CxxGxxR(T/S) and a general-acid catalyst (Asp), the general features of the mechanism involve the cysteine nucleophile attacking the phosphorus atom of the substrate to form a phosphoenzyme intermediate (7, 8). A general acid (conserved aspartic acid residue) donates a proton to the leaving-group oxygen, releasing the dephosphorylated substrate (9–12). Subsequently, the cysteinyl-phosphate intermediate is hydrolyzed by a water molecule to generate inorganic phosphate.

Much of the detailed knowledge concerning the catalytic mechanism of PTPs and DSPs has been deduced from studies utilizing the substrate *para*-nitrophenyl phosphate (*p*NPP). These studies included kinetic isotope effect (KIE) measurements to determine the transition-state structure for the initial phosphoryl transfer from substrate to enzyme. For the DSP *Vaccinia H1*-related (VHR) and the *Yersinia* PTP and PTP1, the measured KIEs for dephosphorylation of *p*NPP support a loose transition state with a large degree of bond cleavage to the leaving group, a metaphosphate-like structure of the transferring phosphoryl group, and little bond formation to the nucleophile. These findings are similar to those of the uncatalyzed aqueous hydrolysis of the dianions of phosphate monoesters (13). For the enzymatic reactions with *p*NPP, KIEs in the leaving group are consistent with neutralization of charge in the transition state by proton transfer. However, a fundamental question not addressed with the previous KIEs is how DSPs catalyze alkyl phosphate ester (phosphoserine/

<sup>†</sup> This work was supported by NIH Grant (GM47297) to A.C.H. and by NIH Grant (GM59785) to J.M.D.

\* To whom correspondence should be addressed: Department of Biomolecular Chemistry, University of Wisconsin—Medical School, 1300 University Ave, Madison, WI 53706. Phone: 608-265-1859. Fax: 608-262-5253. E-mail: jmdenu@wisc.edu (J.M.D.); Department of Chemistry and Biochemistry, Utah State University, Logan, UT 84322. Phone: 435-797-3442. E-mail: hengge@cc.usu.edu (A.C.H.).

<sup>‡</sup> These authors contributed equally to this work.

<sup>§</sup> Utah State University.

<sup>||</sup> Oregon Health and Science University.

<sup>⊥</sup> University of Wisconsin.

<sup>1</sup> Abbreviations: PTP, protein tyrosine phosphatase; DSP, dual-specificity phosphatase; MAPK, mitogen-activated protein kinase; *p*NPP, *para*-nitrophenyl phosphate; VHR, *Vaccinia H1*-related; *m*NBP, *meta*-nitrobenzyl phosphate; Tris, tris(hydroxymethyl) aminomethane; Bis-Tris, 2(bis(2-hydroxyethyl)imino)-2-(hydroxymethyl)-1,3-propanediol; KIE, kinetic isotope effect; EIE, equilibrium isotope effect.

threonine) hydrolysis with similar efficiency to that of aryl phosphate esters, such as *p*NPP or phosphotyrosine. For instance, VHR readily hydrolyzes aryl and alkyl phospho- monoesters whose reactivity (leaving-group potential) can vary by as much as 9 orders of magnitude (8, 14). The common phosphatase substrate *p*NPP generates an excellent leaving group (*p*-nitrophenol) with a  $pK_a$  of 7.1, whereas phosphotyrosine and phosphoserine generate leaving groups with  $pK_a$  values of 10 and 14, respectively. How do DSPs compensate for the huge difference in reactivity based on the leaving-group  $pK_a$ ?

Because previous KIEs have been measured with *p*NPP, transition-state information has been limited to aryl substrates with good leaving groups, i.e., low  $pK_a$ . Recently, Grzyska et al. have used *meta*-nitrobenzyl phosphate (*m*NBP, leaving-group  $pK_a = 14.9$ ) to examine the transition-state structure for the solution hydrolysis reaction of this alkyl phosphate ester (15). The results for the hydrolysis of the monoanion of *m*NBP were most consistent with a preequilibrium proton transfer from the phosphoryl group to the ester oxygen atom, followed by rate-limiting P–O(R) bond fission. The transition state for *m*NBP hydrolysis (leaving-group  $pK_a = 14.9$ ) exhibits much less P–O(R) bond fission than the reaction of the more labile *p*NPP (leaving-group  $pK_a = 7.14$ ). This seemingly anti-Hammond behavior results from a weakening of the P–O(R) ester bond induced by protonation, an effect that calculations show to be much more pronounced for aryl phosphates than for alkyl phosphates (16).

To uncover differences in the transition state for the hydrolysis of aryl versus the alkyl esters by DSPs, we analyzed *m*NBP as a substrate for human phosphatase VHR, measured the KIEs, and compared these results with those obtained previously for *p*NPP. Here, we demonstrate that VHR reacts with the dianionic form of *m*NBP. Previous pH analysis of the kinetic parameters showed that *p*NPP must be in the dianionic state for catalysis (12, 13). The magnitudes of the  $^{18}\text{O}$  and solvent deuterium isotope effects in the reactions of *p*NPP and *m*NBP reveal differences in the timing of protonation and P–O fission in the transition states of the alkyl versus the aryl substrate.

## MATERIALS AND METHODS

**Materials.** Alkaline phosphatase from chicken spleen was purchased from Sigma.

Diethyl ether was used as purchased. The bis(cyclohexyl- ammonium) salt of natural abundance and isotopically labeled *m*NBP were synthesized as previously described (15), and *p*NPP was from Sigma as the disodium hexahydrate salt. VHR and the D92N mutant were purified as previously described (12).

**Assays.** For the pH analysis, a three-component buffer system consisting of 0.1 M acetate, 0.05 M Tris [tris-(hydroxymethyl) aminomethane], and 0.05 M Bis-Tris [2(bis-(2-hydroxyethyl)imino)-2-(hydroxymethyl)-1,3-propanediol] was used to maintain a constant ionic strength throughout the pH range examined. All assays were performed at 25 °C. Assays using *p*NPP as a substrate were performed as described previously (12). The initial velocity of *m*NBP hydrolysis was measured using an inorganic phosphate detection assay described previously (17), with slight variation. Briefly, hydrolysis of *m*NBP (0–7 mM) was

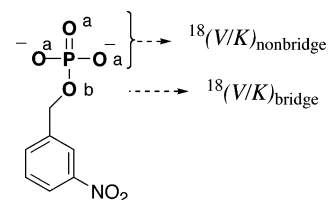


FIGURE 1: Substrate *m*NBP showing the nomenclature for the positions at which isotope effects were measured. Nonbridging oxygen atoms are designated as a, and the bridging oxygen atoms are designated as b.

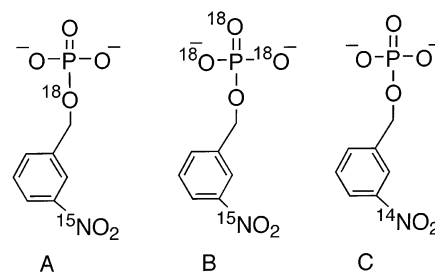


FIGURE 2: Isotopic isomers synthesized for measurement of the bridge (A and C) and nonbridge (B and C)  $^{18}\text{O}$  isotope effects.

initiated by adding VHR (0.16–0.4  $\mu\text{M}$  in a 150- $\mu\text{L}$  reaction volume), and the reaction was quenched with 850  $\mu\text{L}$  of solution containing a 1:6 ratio of 10% ascorbic acid in  $\text{H}_2\text{O}$  and 0.42% ammonium molybdate $\cdot 4\text{H}_2\text{O}$  in 1 N  $\text{H}_2\text{SO}_4$ . The quenched reaction was incubated at 45 °C for 20 min, and the release of phosphate by VHR was detected spectrophotometrically at 820 nm using a Shimadzu BioSpec-1601. The concentration of released phosphate in the reaction was calculated based on a standard curve generated from known concentrations of free phosphate. The data were fitted to eq 1 using the computer program Kaleidagraph (Abelbeck software). For the construction of the pH profiles,  $V/K$  values were determined at various pH values (pH 4.5–9.0) and the pH data were fitted to eq 2 using Kaleidagraph.  $C$  is the pH-independent value of  $V/K$ ,  $H$  is the proton concentration, and  $K_{a1}$ ,  $K_{a2}$ , and  $K_{a3}$  are the ionization constants of the groups involved in the reaction.

$$v = k_{\text{cat}}[E]_0 S / (S + K_m) \quad (1)$$

$$v = C / [(1 + H/K_{a1})(1 + K_{a2}/H)(1 + H/K_{a3})] \quad (2)$$

**Isotope Effect Determinations.** Figure 1 shows the substrate indicating the positions at which isotope effects were measured.  $^{18}\text{O}$  KIEs were measured by isotope ratio mass spectrometry by the remote label method, using the nitrogen atom as a reporter for isotopic fractionation at the bridge or nonbridge oxygen atoms. The experimental procedures used to measure these isotope effects were similar to those previously reported to measure KIEs in phosphoryl transfer reactions in which the leaving group is *p*-nitrophenol (18).

The isotopic isomers of *m*NBP used for measurement of KIEs are shown in Figure 2. A mixture of isotopic isomers A and C was used for determination of  $^{18}k_{\text{bridge}}$ . Isomers B and C were mixed to reconstitute the natural abundance of  $^{15}\text{N}$ , and this mixture was used for determination of  $^{18}k_{\text{nonbridge}}$ . The isotopic abundance of the mixtures was determined by isotope ratio mass spectrometry. The unlabeled compound, containing the natural abundance of  $^{15}\text{N}$ , was used to measure the  $^{15}\text{N}$  isotope effect.

Isotope effect experiments were run at pH 6.0 and 7.15 using 0.2 M Bis-Tris buffer containing 1 mM dithiothreitol, at 30 °C. Temperature was maintained with a thermostated heating block. The dicyclohexylammonium salt (43 mg) of the appropriate isotopically labeled form of the substrate was dissolved in 10 mL of buffer that had been flushed with nitrogen for 30 min before the reaction. Reactions were initiated by addition of 250–350  $\mu\text{L}$  of enzyme (86–113  $\mu\text{M}$ ) and were monitored by  $^{31}\text{P}$  NMR. After partial hydrolysis, reaction mixtures were extracted with diethyl ether 4 times (25 mL) to separate the product *m*-nitrobenzyl alcohol. These ether layers were dried over magnesium sulfate, and the ether was removed by rotary evaporation. The *m*-nitrobenzyl alcohol was further purified by distillation at  $\sim 105$  °C onto a coldfinger apparatus before isotopic analysis by isotope ratio mass spectrometry using an ANCA-NT combustion system working in tandem with a Europa 20-20 isotope ratio mass spectrometer. The aqueous layer, containing the unreacted *m*NBP, was added to Tris buffer and brought to pH  $\sim 9$ . About 1 mg of commercial alkaline phosphatase was added to cleave the residual *m*NBP. After more than 10 half-lives, this mixture was treated as described above to recover *m*-nitrobenzyl alcohol.

Isotope effects were calculated from the isotopic ratios at partial reaction in the product at partial reaction, ( $R_p$ ), in the residual substrate ( $R_s$ ), and in the starting material ( $R_o$ ).

$$\text{KIE} = \log(1 - f) / \log[1 - f(R_p/R_o)] \quad (3)$$

$$\text{KIE} = \log(1 - f) / \log[(1 - f)(R_s/R_o)] \quad (4)$$

Equations 3 and 4 were used to calculate the observed isotope effect either from  $R_p$  and  $R_o$  or from  $R_s$  and  $R_o$ , respectively, at the measured fraction of reaction (19). Experiments using the natural abundance compound showed that there is no measurable  $^{15}\text{N}$  isotope effect. The  $^{18}\text{O}$  isotope effects were corrected for levels of isotopic incorporation, as previously described (15). The independent calculation of each isotope effect using  $R_o$  and  $R_p$  and using  $R_o$  and  $R_s$  from eqs 3 and 4, respectively, provides an internal check of the results.

***D<sub>2</sub>O Solvent Isotope Effect.*** The  $V/K$  values were determined using a buffer consisting of 50 mM Bis-Tris in  $\text{H}_2\text{O}$  or  $\text{D}_2\text{O}$ . Buffer components were added directly to  $\text{D}_2\text{O}$  and the pD was adjusted with NaOD. Assays were performed as described for pH studies in the Materials and Methods. The pD values were determined by adding 0.4 to the pH electrode reading (20).

## RESULTS AND DISCUSSION

First, we examined the ability of VHR to catalyze the hydrolysis of the alkyl phosphate ester *m*NBP with direct comparisons to *p*NPP as a substrate. Initial velocities as a function of *m*NBP concentration were measured, and from the resulting saturation curves (Figure 3), the steady-state kinetic constants were determined at pH 6. Despite the difference of  $\sim 8$   $\text{p}K_a$  units between the leaving groups of *p*NPP ( $\text{p}K_a = 7.1$ ) and *m*NBP ( $\text{p}K_a = 14.9$ ), the  $V/K$  value with *m*NBP was only 2-fold lower than the value obtained with *p*NPP (Figure 4). Similarly, the  $k_{\text{cat}}$  was  $\sim 2$ -fold lower with *m*NBP compared to that with *p*NPP (Figure 3).

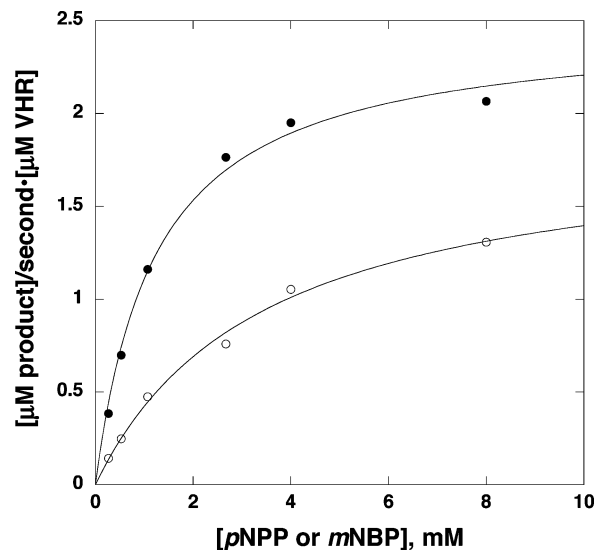


FIGURE 3: Initial velocities of *p*NPP (●) and *m*NBP (○) hydrolysis by VHR were measured at pH 6.0 at 25 °C using the phosphate detection assay as described in the Materials and Methods. The solid lines are fits to the Michaelis–Menten equation. Each point was determined 3 times.

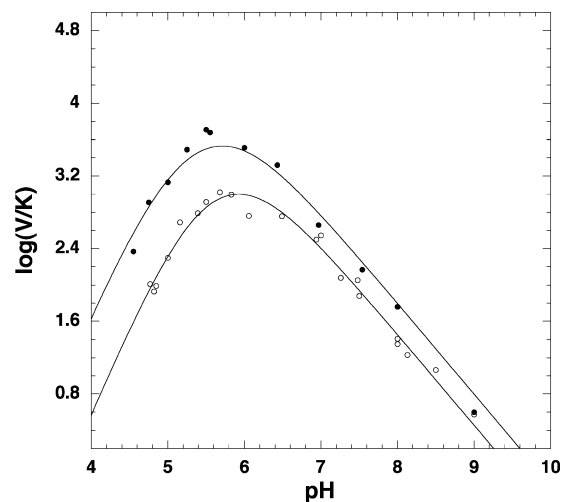


FIGURE 4: pH dependency of the  $V/K$  value for VHR using *p*NPP and *m*NBP. (●) represents the *p*NPP substrate, and (○) represents the *m*NBP substrate. The *p*NPP data are from Denu et al. (12). The data were fitted to eq 2. Assays were performed in TBA buffer (100 mM acetate, 50 mM Bis-Tris, and 50 mM Tris) at 25 °C. See the Materials and Methods for details.

In uncatalyzed hydrolysis reactions, the monoanionic form of an alkyl phosphate is hydrolyzed much faster than the corresponding dianionic form. However, pH analyses of the  $V/K$  values showed that *p*NPP must be in the dianionic state for catalysis by PTPs (12, 13). To examine the formal possibility that similar catalytic efficiencies between *p*NPP and *m*NBP were due to a difference in the initial protonation state of the substrate, it was critical to determine whether the monoanionic or dianionic form of *m*NBP was the catalytically reactive form. Using VHR and *m*NBP, the kinetic parameter  $V/K$  was determined as a function of pH. At each pH value,  $V/K$  values were determined by fitting initial velocities determined at varied [*m*NBP] to the Michaelis–Menten equation (eq 1) as described in the Materials and Methods. The data are presented in Figure 4, along with the previously obtained pH profile for *p*NPP hydrolysis by

VHR (12). Several data points with *p*NPP were reperformed to rule out any significant alterations that might arise from the use of different enzyme preparations. Within experimental error, the current data fell within the previously constructed *V/K* pH profile with *p*NPP. The pH profile with *m*NBP generated a curve that was very similar in its overall shape to that of VHR using *p*NPP, where the plot rises with a slope of +2 on the acidic side and decreases with a slope of -1 on the basic side (Figure 4). However, the *m*NBP pH profile is shifted significantly toward higher pH values on the acidic limb of the profile. Consistent with previous interpretations, the plot indicates that two ionizable groups must be unprotonated and one group must be protonated for optimal activity. From previous analysis with *p*NPP (12), it was determined that two groups with  $pK_a$  values of 5.1 and 5.47 must be unprotonated, while a group with a  $pK_a$  value of 5.7 must be protonated for activity. The  $pK_a$  value of 5.1 represents  $pK_2$  for the phosphate group of *p*NPP and indicates that the dianion of *p*NPP is the reactive form of the substrate. The  $pK_a$  of 5.47 represents the catalytic cysteine (Cys-124) residue, and  $pK_a$  of 5.7 represents the aspartic acid residue (Asp-92) of VHR (12).

When the substrate naphthyl phosphate is employed instead of *p*NPP for the YOP PTP, a similar pH-dependent rate shift was observed, consistent with the difference expected from the second  $pK_a$  of the two substrates (21). The second  $pK_a$  of *m*NBP is 6.2 (15), compared with 5.1 for *p*NPP. This suggests that the shift in the profile in the present study reflects a change in the  $pK_2$  of the phosphate from 5.1 to 6.2.

To demonstrate that the shift in the *m*NBP pH profile is consistent with the  $pK_a$  difference between *p*NPP and *m*NBP, the *m*NBP data were fitted to eq 2 using the previously determined values for Asp-92 ( $pK_{a2} = 5.7$ ; must be protonated) and Cys-124 ( $pK_{a3} = 5.47$ ; must be unprotonated) (12). The  $pK_{a1}$  value for the substrate and the *C* value were allowed to float in the analysis, yielding a  $pK_a$  value of 5.7 for the substrate ionization and the pH-independent value *C* of  $5730 \text{ M}^{-1} \text{ s}^{-1}$ . The calculated kinetic  $pK_{a1}$  value of 5.7 is reasonably close to the thermodynamic  $pK_2$  of *m*NBP determined as 6.2. Using the same type of fitting analysis for the *p*NPP data, a fit to eq 2 yielded a  $pK_{a1}$  value of 4.93, which is very similar to the  $pK_2$  of *p*NPP determined as 5.1. The pH-independent value *C* was  $12\,600 \text{ M}^{-1} \text{ s}^{-1}$ . Poor fits ( $\chi^2 > 0.45$  versus 0.2 for the above model) were obtained for alternative models involving one deprotonated and two protonated groups, as well as one model involving one unprotonated and one protonated groups. Moreover, if we assume a model that involves an unprotonated Asp-92 and the monoanion of the substrate, the fit yields a pH-independent value for *m*NBP that is 23-fold lower than that with *p*NPP. Given that the  $k_{\text{cat}}$  values are only ~2-fold different between the two substrates, which is similar to the difference in *V/K* observed from the fit used in Figure 4, this is an unlikely model. Collectively, the pH studies suggest that VHR utilizes the dianionic forms of both *p*NPP and *m*NBP for catalysis.

The data presented above suggest that both *p*NPP and *m*NBP react with VHR as the dianion and that the catalytic efficiency with alkyl esters does not appear to stem from a utilization of the monoanion over the dianion, as might be predicted from solution chemistry. From computational

studies, it has been proposed that alkyl phosphates might be more likely to react via the monoanion form (22, 23), although another computational study by Asthagiri et al. favors the dianion and loose transition-state pathway for PTP catalyzed phosphoenzyme intermediate formation (24).

If the true substrate was the monoanion of *m*NBP, then it may be possible that the proton from the phosphoryl group is transferred to the leaving group, facilitating P–O bond cleavage. In this model, protonation of the leaving group by the general-acid catalyst Asp-92 may be dispensable for activity when sufficient quantities of the monoanion of *m*NBP are present to compensate for the loss of Asp-92. To test this possibility, we determined the ability of the catalytic mutant D92N of VHR (12) to hydrolyze *m*NBP. We attempted to obtain measurable rates of *m*NBP hydrolysis with D92N VHR using the phosphate detection assay as described in the Materials and Methods. Although reasonable rates of hydrolysis were observed with *p*NPP, KIE results show that the leaving group departs as the unprotonated anion (13). With *m*NBP, the reaction rate is below the detection limits of the assay. However, on the basis of the sensitivity of the assay, we calculated an upper limit of  $0.14 \times 10^{-4} \text{ s}^{-1}$  for the rate of *m*NBP hydrolysis, which was ~3.5 orders of magnitude slower than the value of  $0.05 \text{ s}^{-1}$  measured with *p*NPP and the D92N mutant. This value is consistent with that calculated from the Brønsted plot of the  $k_{\text{cat}}$  value for D92N as a function of the leaving-group  $pK_a$  with a series of aryl phosphate esters (8). The resulting Brønsted slope of  $-0.5 \pm 0.07$  predicts a reduction in the rate of ~3.9 orders of magnitude when the leaving group is changed from *p*-nitrophenol to *m*-nitrobenzyl alcohol. Together, these data support a critical role for the Asp-92 in protonating leaving groups with high  $pK_a$  values, such as *m*NBP and phosphoserine/threonine, as previous studies have implied for aryl ester substrates.<sup>2</sup> These data are consistent with the dianion of both *p*NPP and *m*NBP as the catalyzed substrate.

The proposal that a phosphatase should prefer the monoanion form of its substrate comes from the observation that, in uncatalyzed hydrolysis, the monoanion is more reactive than the dianion. However, this difference in reactivity arises from the ability of a proton to easily transfer intramolecularly from the phosphoryl group to the leaving group in the reaction of the monoanion, while in the dianion, the leaving group departs as the alkoxide. Interestingly, the phosphoryl group is fully deprotonated in the transition states of both the monoanion and dianion reactions. The basic elements that facilitate the uncatalyzed monoanion over the dianion reaction are present in an enzymatic reaction when a general acid is available to protonate the leaving group. In the case of the enzymatic reaction, the aspartic acid within the active site supplies the proton that is transferred to the leaving group, obviating the need to obtain the proton from the monoanion.

To probe the transition-state structure for phosphoryl transfer from *m*NBP to VHR, KIEs for the VHR-catalyzed

<sup>2</sup> It is important to note an exception to the required function of the general-acid aspartic acid residue in both PTPs and DSPs. When the leaving-group  $pK_a$  of aryl phosphates drops below ~5, the requirement for general-acid catalysis is lost for these highly labile substrates, whose departing groups leave without protonation. This is also observed in uncatalyzed hydrolysis reactions. With leaving groups below  $pK_a \sim 5.5$ , the dianion form reacts faster than the monoanion form (1, 2).

Table 1: Experimental Values for  $^{18}(V/K)_{\text{bridge}}$  and  $^{18}(V/K)_{\text{nonbridge}}$  with the Standard Errors in the Last Decimal Place(s) in Parentheses

	$^{18}(V/K)_{\text{bridge}}$	$^{18}(V/K)_{\text{nonbridge}}$ (observed)	$^{18}(V/K)_{\text{nonbridge}}$ (assuming the monoanion is the substrate)	$^{18}(V/K)_{\text{nonbridge}}$ (assuming the dianion is the substrate)
<i>m</i> NBP VHR, pH 6.0, 30 °C	1.0004 (7)	1.0078 (3)	1.0137 (3)	0.9986 (3)
<i>m</i> NBP VHR, pH 7.15, 30 °C		1.0004 (6)	1.0141 (6)	0.9989 (6)
<i>m</i> NBP monoanion hydrolysis, pH 4.0, 115 °C	0.9982 (7)	1.0149 (4)		
<i>p</i> NPP VHR, pH 6, 30 °C (13)	1.0118 (20)	1.0019 (3)	1.0156 (3)	1.0003 (3)
<i>p</i> NPP monoanion hydrolysis, pH 3.5, 95 °C	1.0087 (3)	1.0184 (5)		

reaction of *m*NBP were measured and compared with previous data using *p*NPP (Table 1). All of the isotope effects in this study were measured by the competitive method and therefore are isotope effects on  $V/K$ . Thus, these KIEs are those for the phosphoryl transfer from the substrate to form the phosphoenzyme intermediate. Isotope effects were measured at the pH optimum of 6.0, and the value for  $^{18}(V/K)_{\text{nonbridge}}$  was also measured at pH 7.15, where the rate is slower. Because the nonbridge isotope effect is also sensitive to the protonation state of the substrate, the observed value differs but should give the same value for  $^{18}(V/K)_{\text{nonbridge}}$  after the correction for the protonation state of the substrate, if chemistry is fully rate-limiting.

Because the second  $pK_a$  for *m*NBP is 6.2 (15), an equilibrium population of both the monoanion and dianion species are present at both pH values used in the isotope effect experiments. The known  $^{18}\text{O}$  equilibrium isotope effect (EIE) for deprotonation of phosphate esters (1.015) (25) allows for the correction of the observed values of  $^{18}(V/K)_{\text{nonbridge}}$  for this fractionation. The proper correction requires an assumption as to whether the substrate for catalysis is the monoanion or the dianion. While the experimental evidence discussed above indicates that the substrate is the dianion, we have corrected the observed  $^{18}(V/K)_{\text{nonbridge}}$  KIE in Table 1 assuming both possibilities, in an effort to examine whether the data favor one case or the other, independent of the kinetic data supporting the notion that the reactive form of the substrate is the dianion.

In the generally accepted mechanism for the uncatalyzed hydrolysis of the monoanion of phosphate esters, the proton is transferred from the phosphoryl group to the leaving group either in the transition state or in a preequilibrium step. The  $^{18}k_{\text{nonbridge}}$  for the hydrolysis of the monoanion of *m*NBP reflects the deprotonation of the phosphoryl group. In contrast, in reactions of the dianion of a phosphate ester, the  $^{18}k_{\text{nonbridge}}$  is very small and inverse, reflecting the loose transition state involving no proton transfers to or from the phosphoryl group. Because of the extremely slow rate of the uncatalyzed hydrolysis of the dianions of alkyl phosphate esters (26), the KIEs for the reaction of the dianion of *m*NBP could not be measured. Experimental evidence indicates that alkyl phosphate dianions undergo hydrolysis by a mechanism and transition state similar to aryl phosphates (26), and thus, the reaction of the dianion of *m*NBP would be expected to exhibit a small inverse  $^{18}k_{\text{nonbridge}}$  similar to that for the dianion of *p*NPP (0.9994).

Correction of the observed value of  $^{18}(V/K)_{\text{nonbridge}}$ , assuming the catalytically active species is the monoanion, results in values of  $1.0137 \pm 0.0003$  at pH 6.0 and  $1.0144 \pm 0.0006$  at pH 7.15. Both values are very similar to that obtained for the hydrolysis of the monoanion in solution. Similarly, the correction assuming the dianion is the reactive species results in very small inverse values, expected if the transition state

is loose, as supported by prior experiments. Thus, the  $^{18}(V/K)_{\text{nonbridge}}$  KIEs do not distinguish whether the monoanion or the dianion is the substrate. Although the KIEs cannot distinguish these two possibilities, the kinetic data described above strongly point to the dianion as the reactive form of the substrate. If the monoanion is the substrate, the similarity of  $^{18}(V/K)_{\text{nonbridge}}$  to the full EIE for deprotonation indicates that this proton is essentially fully removed in the transition state. In this mechanistic scenario, the phosphoryl group of the substrate serves as the source of the proton that is transferred to the leaving group. However, the failure to observe a measurable rate of hydrolysis of *m*NBP with the D92N mutant indicates that it is this residue and not the phosphoryl group of the substrate that supplies the proton to the leaving group. It has been proposed that the carboxylate form of this residue merely provides stabilization of a bridge-protonated substrate. If this was the only role for this residue and the proton source is the substrate, then one would expect a similar leaving-group dependency in the D92N mutant as for the uncatalyzed reaction. However, the measured Brønsted slope of  $-0.5$  is significantly larger than that for the uncatalyzed hydrolysis ( $-0.2$ , ref 1). Moreover, the monoanion as the substrate is also inconsistent with the pH-rate analysis that shows that two groups must be deprotonated.

The  $^{18}(V/K)_{\text{bridge}}$  KIE of 1.0004 is much smaller than that for the reaction using *p*NPP as the substrate. It seems counterintuitive that a KIE at a position of bond fission in the *m*NBP reaction does not result in a significant normal value. This unexpected KIE difference is also observed in the uncatalyzed hydrolysis of the monoanions of these two esters and can be explained by the relative contributions from the inverse isotope effect for protonation and the normal one for P–O(R) bond fission. The difference between the values for *p*NPP and *m*NBP reveals differences arising from the timing of these events in the uncatalyzed hydrolysis (15) and perhaps in the enzymatic reaction as well.

In the reactions of both substrates, the observed  $^{18}(V/K)_{\text{bridge}}$  is the product for P–O ester bond fission and for protonation. In the case of *p*NPP, these maximal values are 1.034 and 0.985, respectively (18). With the alkyl ester *m*NBP, the isotope effect maxima may be larger. Leaving-group  $^{18}\text{O}$  KIEs of up to 1.062 have been reported for the hydrazinolysis of methyl formate, when breakdown of the tetrahedral intermediate is rate-limiting (27). Ab initio calculations predict a similar maximum value for methyl phosphate (unpublished results). The isotope effect for protonation may be estimated from the protonation of hydroxide, which is 0.96 (28). Whatever the precise values, the most important fact is that the magnitude of the isotope effect for P–O fission exceeds that of protonation, which is logical because the phosphate ester involves bending and torsional modes lost when the phosphoryl group is replaced by hydrogen. For the same

reason,  $^{18}\text{O}$  fractionation factors between water and alcohols are 2–3% normal (29) and the EIE for deacetylation of *p*-nitrophenyl acetate (1.0277) is larger than the EIE for deprotonation of *p*-nitrophenol (1.015) (30).

Thus, the significant normal  $^{18}(\text{V}/\text{K})_{\text{bridge}}$  in the *p*NPP reaction requires that P–O fission be equal to or ahead of proton transfer. The absence of a significant  $^{15}(\text{V}/\text{K})$  with this substrate indicates that no significant negative charge resides on the leaving group in the transition state, implying that proton transfer must be approximately as far advanced as P–O bond fission. With the *m*NBP substrate, the negligible  $^{18}(\text{V}/\text{K})_{\text{bridge}}$  (Table 1) requires that these two contributions cancel, which is only possible if protonation is ahead of P–O bond fission. If the reverse were true or if both processes are equally progressed in the transition state, a normal  $^{18}(\text{V}/\text{K})_{\text{bridge}}$  would result.

Previously reported KIE results on the uncatalyzed hydrolysis of *m*NBP indicate a similar difference in P–O(R) bond fission between the aryl and alkyl phosphate ester substrates (15). In that case, small inverse solvent isotope effects of 0.94 were observed with both *m*NBP and *p*NPP, which were attributed to proton transfer occurring in a step before P–O ester bond fission. Could protonation of the ester oxygen atom also occur in a distinct step of the VHR-catalyzed reaction, rather than occurring simultaneously with P–O(R) bond fission? In such a scenario, proton transfer could occur from Asp-92, the reported general acid, and the resulting carboxylate group could stabilize the bridge-protonated form of the substrate, which has been proposed on computational grounds (23).

To examine the possibility that protonation and P–O bond fission might be stepwise or at least asynchronous with protonation ahead of P–O scission, the solvent deuterium isotope effect on *V/K* was measured for the VHR-catalyzed hydrolysis of *m*NBP. The classic general-acid mechanism, with a proton in flight in the transition state of the rate-limiting step, typically results in a normal solvent KIE. Its magnitude depends on the transition state for proton transfer, with the largest values observed for symmetric transition states; a reaction in which the transition state is either very early or late can result in a negligible solvent KIE (31). In addition, a stepwise mechanism, in which P–O bond fission is rate-limiting and occurs after proton transfer, would exhibit only an equilibrium isotope effect, which on the basis of the fractionation factors of the species involved, would be inverse. In the VHR reaction, contributors to the observed solvent KIE would be the fractionation factors of the following species: (a) the ionized Cys-124 (from 0.48 to 0.7, ascribed to a medium effect involving hydrogen bonding between the thiolate and solvating water); (b) the bridge-protonated substrate, which may be estimated by that of hydronium ion,  $\sim 0.7$ ; (c) carboxylate (Asp-92), which is near unity (20, 32).

An important caveat is that solvent isotope effects on enzymatic reactions can also arise from viscosity effects, small global effects on structure, and  $\text{pK}_a$  shifts. To minimize such complications, we performed a pL (pD or pH)-dependent analysis of the solvent isotope effects on *V/K* and compared these values between *p*NPP and *m*NBP. The *V/K* values for both *p*NPP (Figure 5A) and *m*NBP (Figure 5B) were determined over a range of pL, so that the maximum value could be easily ascertained from the pL profile, avoiding

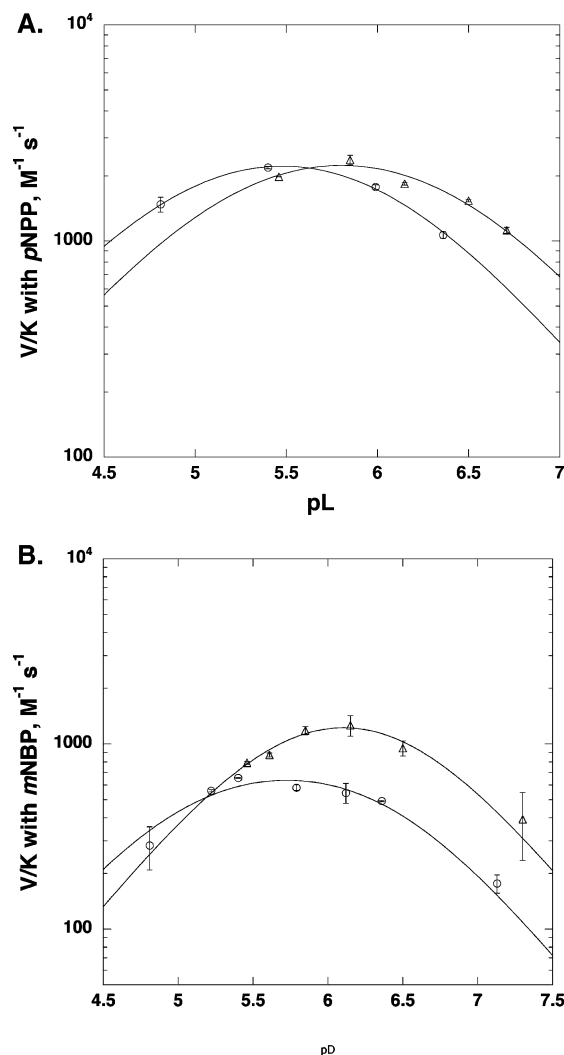


FIGURE 5: Solvent KIEs of VHR-catalyzed hydrolysis of (A) *p*NPP and (B) *m*NBP in  $\text{H}_2\text{O}$  (O) and  $\text{D}_2\text{O}$  ( $\Delta$ ). Hydrolyses of *p*NPP and *m*NBP were assayed in  $\text{H}_2\text{O}$  or  $\text{D}_2\text{O}$  consisting of 50 mM Bis-Tris from pL 4.5 to 7.5 at 25 °C. Error bars are standard deviations from no less than 3 separate determinations. Solid lines are the resulting fits to a bell-shaped pH profile. See the Materials and Methods for details.

any differences in rates that were simply due to shifts in  $\text{pK}_a$  values between the two solvents. With *p*NPP, the solvent isotope effect  $^{\text{D}}\text{V}/\text{K}$  was very small and slightly inverse at  $0.92 \pm 0.05$ . However, with *m*NBP, the  $^{\text{D}}\text{V}/\text{K}$  value was larger and inverse at  $0.52 \pm 0.07$ . Both values were calculated from the peaks of the two plots (parts A and B of Figure 5). Zhang et al. (14) reported a large inverse solvent effect using *p*NPP and VHR and suggested a preequilibrium protonation of the ester oxygen. However, because their solvent effect was measured at a single pL value and by a different assay, it is difficult to compare their value with the values reported here. Our use of both *p*NPP and *m*NBP, as well as performing a thorough pL dependence on the *V/K* values, negates many, if not all, of the potential complications discussed above.

These inverse  $^{\text{D}}\text{V}/\text{K}$  values are consistent with either a very early or late transition state for proton transfer or a mechanism in which the proton is not in flight in the transition state of the rate-limiting step. There is precedent for a very early or late transition state to result in a very small primary KIE masked by inverse EIEs to give an inverse observed

effect. The acid-catalyzed hydrolysis of *ortho*-esters has been shown to be general-acid catalyzed (33). This reaction, like the one under discussion here, involves protonation of the leaving group (34, 35) and has an observed solvent KIE of 0.7 (34). This was ascribed to a KIE of near unity in a very late transition state for proton transfer and an inverse secondary EIE (35).

Interestingly, there is a difference in the magnitude of the solvent isotope effect between the two substrates in the enzymatic reaction (Figure 5), while in the uncatalyzed hydrolysis of the monoanion, there is no difference. The different solvent isotope effects between the two substrates might result from differences in the timing of proton transfer in the enzymatic reaction, such that in the VHR-catalyzed *p*NPP reaction, a normal KIE component from proton transfer might partially offset the inverse solvent EIE. For the reasons described above, an inverse solvent  $^D V/K$  is not sufficient to identify whether proton transfer occurs in a discrete step or in the same step as P–O fission. However, the combined  $^D V/K$  and  $^{18} V/K$  data limit the mechanistic possibilities.

The observation of small inverse solvent KIEs in the uncatalyzed reactions of the monoanions of *p*NPP and *m*NBP but a normal solvent KIE for the reaction of 2,4-dinitrophenyl phosphate suggests that only when the leaving-group  $pK_a$  drops to around 4 does proton transfer occur in the rate-limiting step. If the same is true for the VHR-catalyzed reaction and the ester oxygen is protonated by Asp-92 before P–O fission (with stabilization of this species by the Asp carboxylate) for both *p*NPP and *m*NBP, then  $^D V/K$  is solely an EIE and should be inverse. The 0.52  $^D V/K$  for the reaction of *m*NBP is in the range expected, but the less inverse value of 0.92 with *p*NPP is not expected. The different  $^D V/K$  values indicate that there is a difference in protonation in the transition states of the two reactions.

Protonation of the bridge oxygen atom produces an inverse contribution to  $^{18}(V/K)_{\text{bridge}}$ , and the different  $^{18}(V/K)_{\text{bridge}}$  KIE for the two substrates confirms the differences in the transition states of the two reactions, either from distinct extents of P–O bond fission, in the timing of proton transfer, or both.

The transition state for proton transfer must be either very early or late to account for an inverse, instead of the expected normal, solvent  $^D V/K$ . The ester oxygen is an extremely weak base, making proton transfer unfavorable, which is expected to result in a late transition state. An early transition state would be expected for a thermodynamically favorable proton transfer, which would be the case if P–O bond fission were well-ahead of proton transfer. The notion that P–O bond fission is ahead of and drives proton transfer is not supported by several observations. First, the  $^{15} V/K$  of unity in the VHR-catalyzed reaction of *p*NPP implies that the leaving group does not bear a significant negative charge in the transition state. Second, such a mechanism should manifest itself in a strong dependency of the rate on the leaving-group basicity, while in fact, only a  $\sim 2$ -fold difference in  $V/K$  between *p*NPP and *m*NBP is found. Thus, a late transition state for proton transfer is more likely than an early one, given these considerations.

The near-unity  $^{18}(V/K)_{\text{bridge}}$  KIE with *m*NBP suggests a transition state in which the inverse contribution from protonation cancels the normal contribution from P–O fission. For this to occur, proton transfer must be ahead of

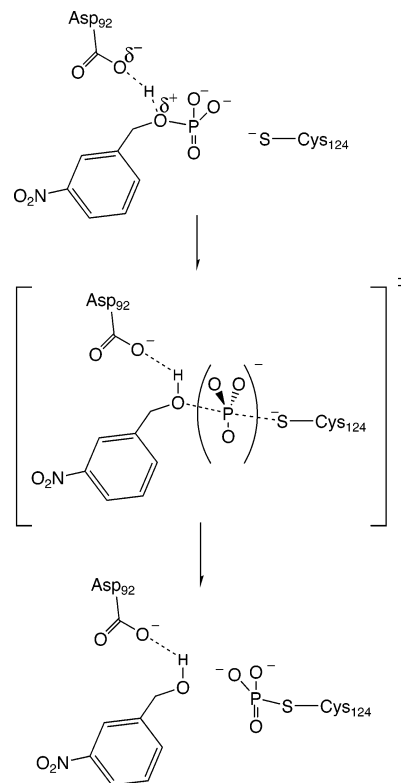


FIGURE 6: Proposed transition state for VHR-catalyzed formation of the cysteinyl-phosphate enzyme intermediate from *m*NBP. Top figure shows an initial protonation step of the ester oxygen by Asp-92 (VHR numbering). Middle figure represents a dissociative (loose) transition state, where P–O cleavage is nearly complete and the proton is already transferred from Asp-92. Bottom figure shows the resulting phosphoenzyme intermediate generated from the nucleophile thiolate anion of Cys-124. Not pictured is the conserved Arg-133, which interacts with two oxygens of phosphate. A concerted process is also consistent with the data, even though proton transfer is required to be ahead of P–O bond fission.

P–O fission because of the larger magnitude of the contribution from P–O bond fission. The *m*NBP data would be consistent with either a preequilibrium proton transfer or a general-acid mechanism. In contrast, for the *p*NPP reaction, the normal KIE implies P–O fission is more synchronous with proton transfer. (In fact, the  $^{18}(V/K)_{\text{bridge}}$  in this reaction is close to that expected if both processes are far advanced.)

A difference in timing of proton transfer in a general-acid mechanism with the two substrates may explain the difference in  $^D V/K$  with the two substrates. The inverse contribution to  $^D V/K$  from the fractionation factor for the nucleophilic Cys will be offset by a normal kinetic effect for the proton in flight. If protonation is far advanced in the transition state of the *m*NBP reaction, the kinetic contribution will be very small and the inverse fractionation factor will be more fully expressed. In the reaction with *p*NPP, if proton transfer is not as far advanced and is more synchronous with P–O fission, a larger normal kinetic contribution to  $^D V/K$  is expected, canceling the inverse EIE and giving the observed  $^D V/K$  near-unity. This is a sensible expectation from the relative basicities of the leaving groups of the two substrates. Proton transfer to the leaving group will become more favorable as the P–O bond breaks. The more basic *m*-nitrobenzyl alkoxy moiety will attain sufficient basicity to make proton transfer more favorable earlier in the reaction coordinate for P–O fission than *p*-nitrophenoxy.

DSPs, as well as some PTPs, may allow for complementarity between leaving-group lability, basicity of the ester oxygen, and timing of proton transfer by aspartic acid, such that there is a continuum that falls between a stepwise and partially concerted mechanism for proton transfer and P–O cleavage and ultimately leads to the similarity in the rates of ester hydrolysis. This basic idea was originally proposed by Kirby and Varvoglis in 1967 (1).

In summary, the results support an enzymatic mechanism that employs the dianionic form of *m*NBP as the substrate and where a proton donated by the acid (Asp-92 in VHR) is transferred to the ester oxygen either in a step prior to significant P–O bond cleavage or in a concerted but asynchronous mechanism in which protonation is well-advanced in the transition state and ahead of P–O bond fission (Figure 6). In contrast, in the VHR-catalyzed *p*NPP reaction, proton transfer to the leaving group and P–O bond fission are probably more synchronous. Even though the dianion is the enzymatic substrate, uncatalyzed monoanion hydrolysis shares the common feature of proton transfer to the leaving group and an unprotonated phosphoryl group in the transition state. The enzymatic data reveal differences in the position on the reaction coordinates of proton transfer and P–O fission in the transition states for the aryl and alkyl substrates. Although calculations suggest that protonation weakens aryl phosphates more than alkyl phosphates, the higher basicity of the alkyl phosphates makes protonation more favorable, perhaps allowing VHR to better match leaving-group potential with the timing of the proton transfer to the ester oxygen, permitting aryl and alkyl phosphoesters to be turned over with similar catalytic efficiency.

## ACKNOWLEDGMENT

We thank W. W. Cleland for critical discussions.

## REFERENCES

- Kirby, A. J., and Varvoglis, A. G. (1967) *J. Am. Chem. Soc.* 89, 415–423.
- Cleland, W. W., and Hengge, A. C. (1995) Mechanisms of phosphoryl and acyl transfer, *FASEB J.* 15, 1585–1594.
- Keyse, S. M. (2000) Protein phosphatases and the regulation of mitogen-activated protein kinase signalling, *Curr. Opin. Cell Biol.* 12, 186–192.
- Neel, B. G., and Tonks, N. K. (1997) Protein tyrosine phosphatases in signal transduction, *Curr. Opin. Cell Biol.* 9, 193–204.
- Tonks, N. K., and Neel, B. G. (2001) Combinatorial control of the specificity of protein tyrosine phosphatases, *Curr. Opin. Cell Biol.* 13, 182–195.
- Denu, J. M., and Dixon, J. E. (1998) Protein tyrosine phosphatases: Mechanisms of catalysis and regulation, *Curr. Opin. Chem. Biol.* 2, 633–641.
- Pannifer, A. D., Flint, A. J., Tonks, N. K., and Barford, D. (1998) Visualization of the cysteinyl-phosphate intermediate of a protein-tyrosine phosphatase by X-ray crystallography, *J. Biol. Chem.* 273, 10454–10462.
- Denu, J. M., Lohse, D. L., Vijayalakshmi, J., Saper, M. A., and Dixon, J. E. (1996) Visualization of intermediate and transition-state structures in protein-tyrosine phosphatase catalysis, *Proc. Natl. Acad. Sci. U.S.A.* 93, 2493–2498.
- Denu, J. M., and Dixon, J. E. (1995) A catalytic mechanism for the dual-specific phosphatases, *Proc. Natl. Acad. Sci. U.S.A.* 92, 5910–5914.
- Lohse, D. L., Denu, J. M., Santoro, N., and Dixon, J. E. (1997) Roles of aspartic acid-181 and serine-222 in intermediate formation and hydrolysis of the mammalian protein-tyrosine-phosphatase PTP1, *Biochemistry* 36, 4568–4575.
- Zhang, Z. Y., Wang, Y., and Dixon, J. E. (1994) Dissecting the catalytic mechanism of protein-tyrosine phosphatases, *Proc. Natl. Acad. Sci. U.S.A.* 91, 1624–1627.
- Denu, J. M., Zhou, G., Guo, Y., and Dixon, J. E. (1995) The catalytic role of aspartic acid-92 in a human dual-specific protein-tyrosine-phosphatase, *Biochemistry* 34, 3396–3403.
- Hengge, A. C., Denu, J. M., and Dixon, J. E. (1996) Transition-state structures for the native dual-specific phosphatase VHR and D92N and S131A mutants. Contributions to the driving force for catalysis, *Biochemistry* 35, 7084–7092.
- Zhang, Z.-Y., Wu, L., and Chen, L. (1995) Transition state and rate-limiting step of the reaction catalyzed by the human dual-specificity phosphatase, VHR, *Biochemistry* 34, 16088–16096.
- Grzyska, P. K., Czyryca, P. G., Purcell, J., and Hengge, A. C. (2003) Hydrolysis reactions of alkyl versus aryl phosphate monoester monoanions, *J. Am. Chem. Soc.* 125, 13106–13111.
- Bianciotto, M., Barthelat, J.-C., and Vigroux, A. (2002) Reactivity of phosphate monoester monoanions in aqueous solution. 2. A theoretical study of the elusive zwitterion intermediates  $\text{RO}^+-\text{(H)PO}_3^{2-}$ , *J. Phys. Chem.* 106, 6521–6526.
- Ames, N. A., and Dubin, D. T. (1960) The role of polyamine in the neutralization of bacteriophage deoxyribonucleic acid, *J. Biol. Chem.* 235, 769–775.
- Hengge, A. C. (2002) Isotope effects in the study of phosphoryl and sulfuryl transfer reactions, *Acc. Chem. Res.* 35, 105–112.
- Bigeleisen, J., and Wolfsberg, M. (1958) Theoretical and experimental aspects of isotope effects in chemical kinetics, *Adv. Chem. Phys.* 1, 15–76.
- Schowen, K. B., and Schowen, R. L. (1982) Solvent isotope effects of enzyme systems, *Methods Enzymol.* 87, 551–606.
- Zhang, Z.-Y., Malachowski, W. P., Van Etten, R. L., and Dixon, J. E. (1994) Nature of the rate-determining steps of the reaction catalyzed by the Yersinia protein-tyrosine phosphatase, *J. Biol. Chem.* 269, 8140–8145.
- Kolmodin, K., Nordlund, P., and Aqvist, J. (1999) Mechanism of substrate dephosphorylation in low Mr protein tyrosine phosphatase, *Proteins: Struct., Funct., Genet.* 36, 370–379.
- Hart, J. C., Hillier, I. H., Burton, N. A., and Sheppard, D. W. (1998) An alternative role for the conserved Asp residue in phosphoryl transfer reactions, *J. Am. Chem. Soc.* 120, 13535–13536.
- Asthaigiri, D., Dillet, V., Liu, T., Noodleman, L., Van Etten, R. L., and Bashford, D. (2002) Density functional study of the mechanism of a tyrosine phosphatase: I. Intermediate formation, *J. Am. Chem. Soc.* 124, 10225–10235.
- Knight, W. B., Weiss, P. M., and Cleland, W. W. (1986) Determination of equilibrium  $^{18}\text{O}$  isotope effects on the deprotonation of phosphate and phosphate esters and the anomeric effect on deprotonation of glucose-6-phosphate, *J. Am. Chem. Soc.* 108, 2759–2761.
- Lad, C., Williams, N. H., and Wolfenden, R. (2003) The rate of hydrolysis of phosphomonoester dianions and the exceptional catalytic proficiencies of protein and inositol phosphatases, *Proc. Natl. Acad. Sci. U.S.A.* 100, 5607–5610.
- Sawyer, C. B., and Kirsch, J. F. (1973) Kinetic isotope effects for reactions of methyl formate-methoxyl- $^{18}\text{O}$ , *J. Am. Chem. Soc.* 95, 7375–7381.
- Green, M., and Taube, H. (1963) Isotopic fractionation in the  $\text{OH}^-$ - $\text{H}_2\text{O}$  exchange reaction, *J. Phys. Chem.* 67, 1565–1566.
- Rishavy, M. A., and Cleland, W. W. (1999)  $^{13}\text{C}$ ,  $^{15}\text{N}$ , and  $^{18}\text{O}$  equilibrium isotope effects and fractionation factors, *Can. J. Chem.* 77, 967–977.
- Hengge, A. C., and Hess, R. A. (1994) Concerted or stepwise mechanisms for acyl transfer reactions of *p*-nitrophenyl acetate? Transition state structures from isotope effects, *J. Am. Chem. Soc.* 116, 11256–11263.
- Melander, L., and Saunders, W. H. (1987) *Reaction Rates of Isotopic Molecules*, pp 130–139, Robert E. Krieger, Malabar, FL.
- Quinn, D. M., and Sutton, L. D. (1991) in *Enzyme Mechanism from Isotope Effects* (Cook, P. F., Ed.) pp 73–126, CRC Press, Boca Raton, FL.
- Fife, T. H. (1972) General acid catalysis of acetal, ketal, and ortho ester hydrolysis, *Acc. Chem. Res.* 5, 264–272.
- Jencks, W. P. (1987) *Catalysis in Chemistry and Enzymology*, Dover Publications, Inc, New York.
- Kresge, A. J., and Preto, R. J. (1965) The mechanism of hydrolysis of ortho esters, *J. Am. Chem. Soc.* 87, 4593.